9/17/86 Jack Daemen
Daeman
Prof.
UNR

Constitutive Relations - (Rock) Material Behavior Models

(Stress-strain relations)

(Thermodynamic equations of state)

Examples:
- (linear) elasticity
- (elasto) plasticity
- thermoelasticity
- viscoelasticity

Special case: salt behavior (creep)

Failure criteria: rock mass strength

Problems:
- size effects
  discontinuities
- shape effects
  pillars; confinement
- (apparent) time effects
  strain rate (loading rate)
  load duration
  rock alteration (weathering)

flac codes distributed 3/m

Application: underground opening stability

Lining streams tunnels in Milwaukee

Mark Board

think of complex of flac creep laws for

Review the 8 creep laws

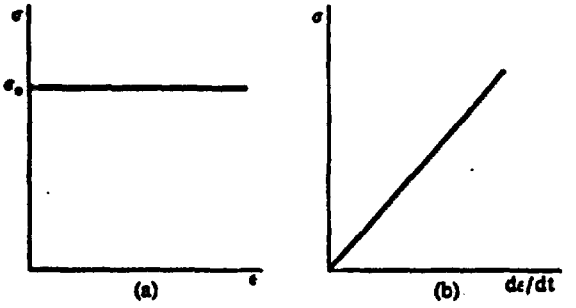

Figure 1.18. Stress-strain, and stress-strain rate curves for (*a*) perfectly plastic and (*b*) viscous substances.

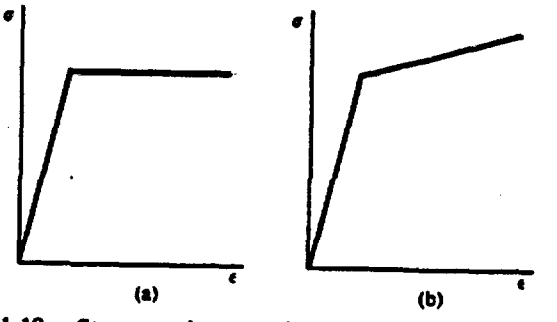

Figure 1.19. Stress-strain curves for (*a*) an elasto-plastic material and (*b*) an elasto-plastic material with strain hardening.

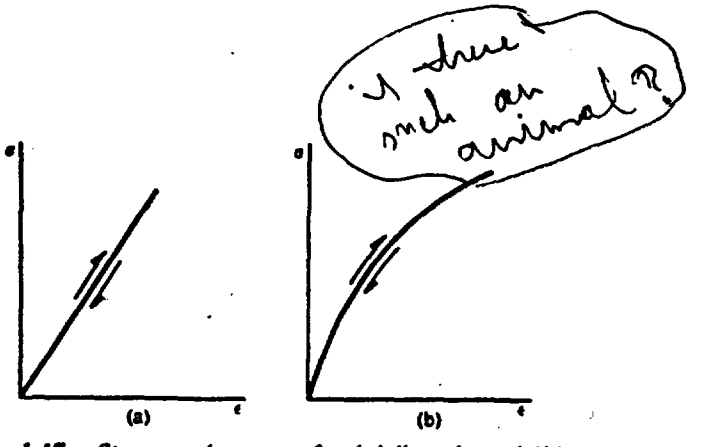

Figure 1.17. Stress-strain curves for (*a*) linearly and (*b*) non-linearly elastic substances.

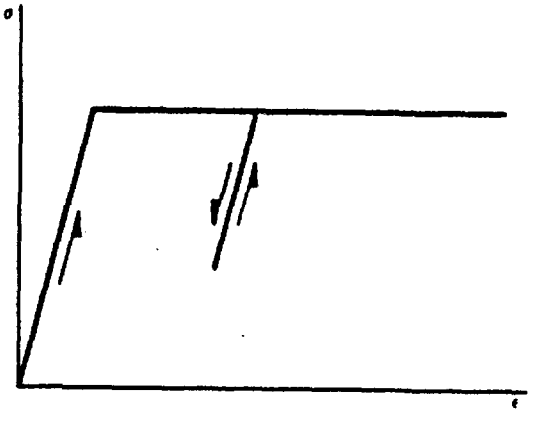

Figure 1.23. Stress-strain curve showing loading and unloading paths for an elasto-plastic material.

From: Budavari, S., 1983, Fundamental Principles of Solid Mechanics, Ch. 1 in Rock Mechanics in Mining Practice, S. Budavari, Editor, The South African Institute of Mining and Metallurgy, Johannesburg.

"Creep Laws"

1. Empirical - curve fitting

2. Rheology - flow/solid mechanism modeling

3. Physical (micro-deformation)

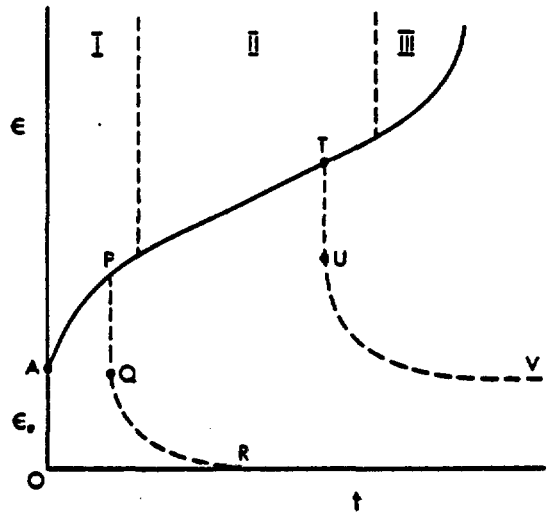

Fig. 11.1.1

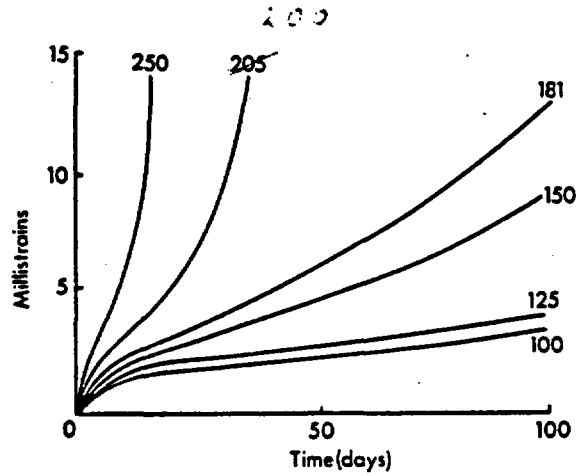

Fig. 11.1.2 Creep of alabaster in water (after Griggs, 1940). Numbers on the curves are values of the uniaxial compressive stress in bars.

From: Jaeger, J.C. and N.G.W. Cook, 1979, Fundamentals of Rock Mechanics, Third Edition, Chapman and Hall, London.

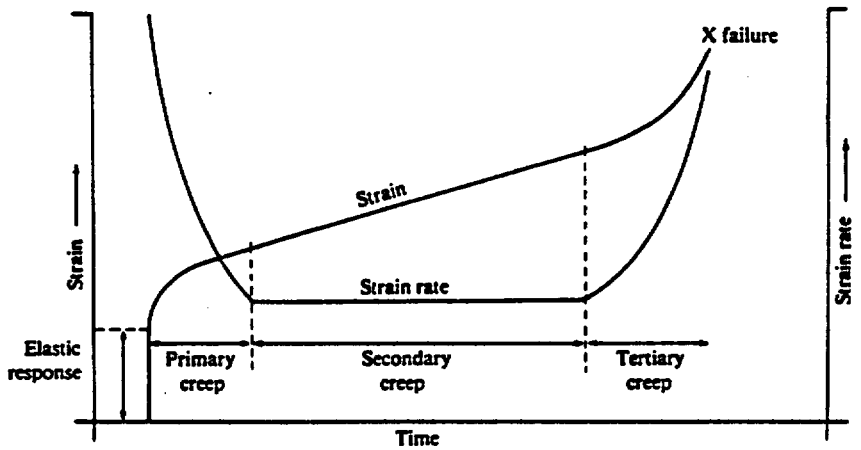

Figure 2.2. Idealized strain-time ('creep') and strain rate-time curves.

From: Patchet, S.J., 1983, Mechanical Properties of Rock and Rock Masses, Ch. 2 in Rock Mechanics in Mining Practice, S. Budavari, Editor, The South African Institute of Mining and Metallurgy, Monograph Series No. 5, Johannesburg.

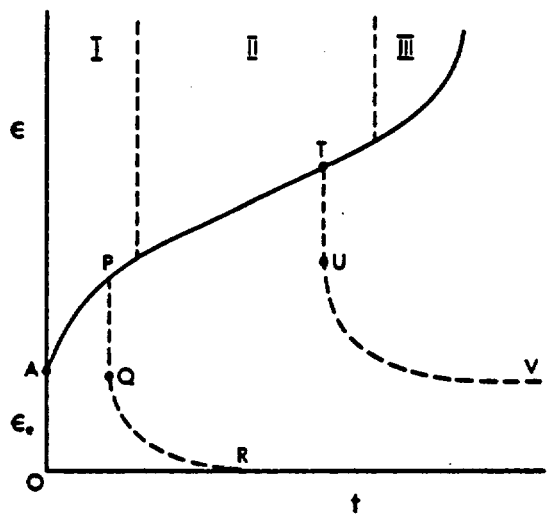

Fig. 11.1.1

From: Jaeger, J.C. and N.G.W. Cook, 1979, Fundamentals of Rock Mechanics, Third Edition, Chapman and Hall, London.

Simple Rheological Models

(a) (b)

Fig. 11.3.1

Hookean spring Newtonian dashpot

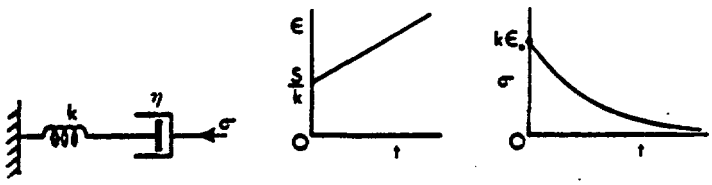

(a) (b) (c)

Fig. 11.3.2

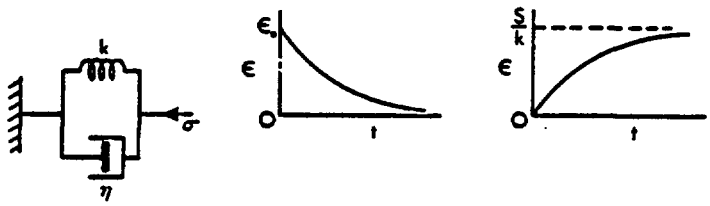

(a) (b) (c)

Fig. 11.3.3

Maxwell; elastico-viscous Kelvin, Voigt; firmo-viscous

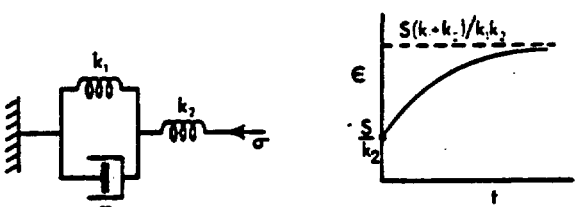

(a) (b)

Fig. 11.3.4

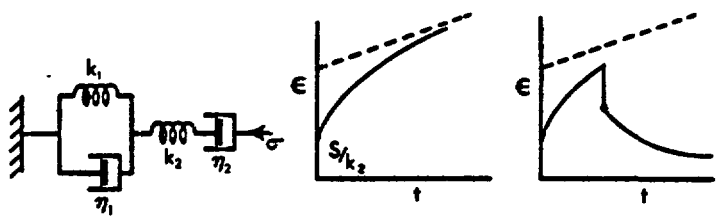

(a) (b) (c)

Fig. 11.3.5

Generalized Kelvin Burgers

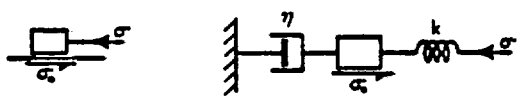

(a) (b)

Fig. 11.3.6

Bingham

From: Jaeger, J.C. and N.G.W. Cook, 1979, Fundamentals of Rock Mechanics, Third Edition, Chapman and Hall, London.

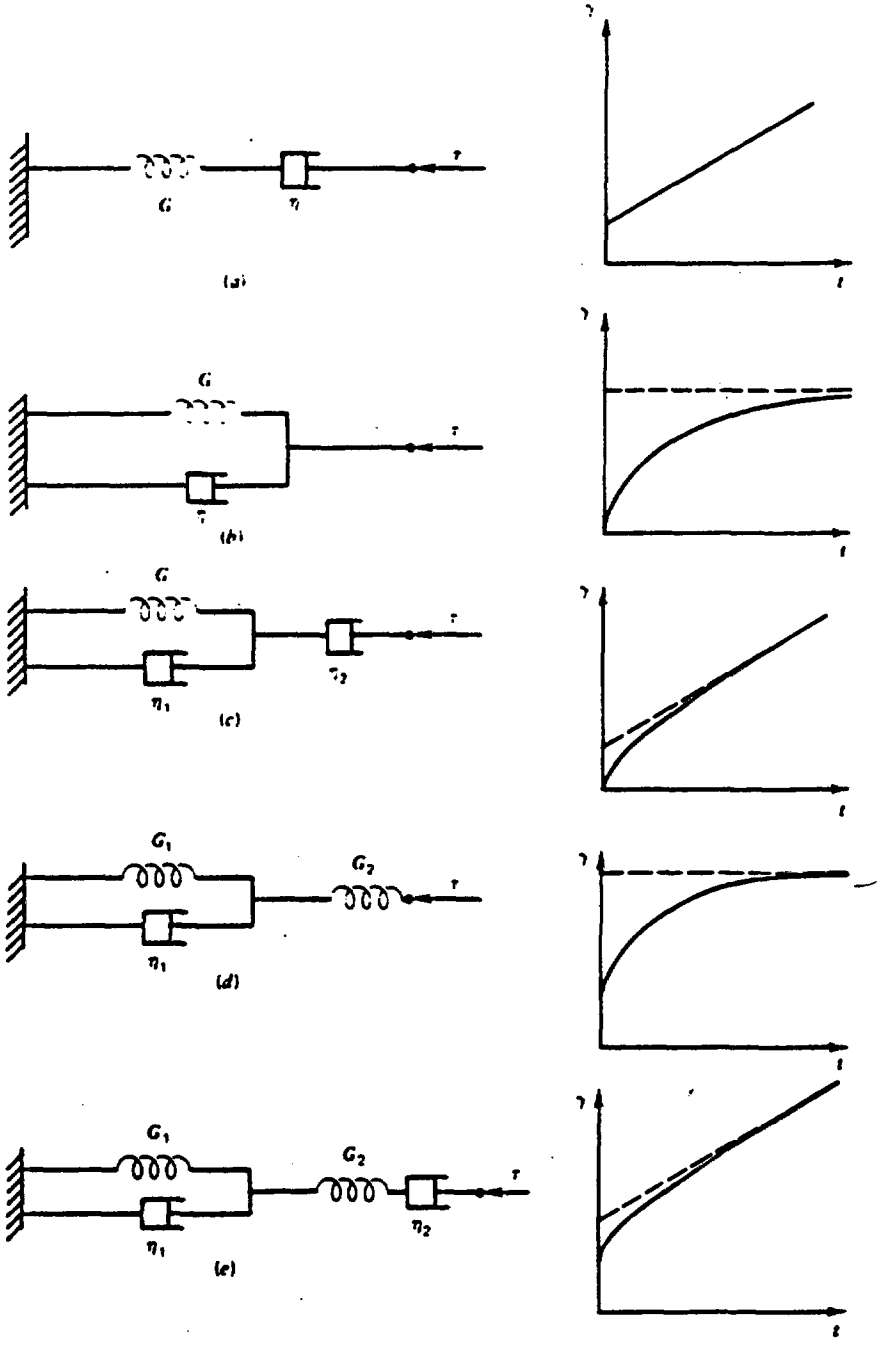

Figure 6.17 Simple linear viscoelastic models and their response to the creep test. (*a*) Two-constant liquid (Maxwell body). (*b*) Two-constant solid (Kelvin body). (*c*) Three-constant liquid (generalized Maxwell body). (*d*) Three-constant solid. (*e*) Four-constant liquid (Burgers body).

From: R.E. Goodman, 1980, Introduction to Rock Mechanics, John Wiley and Sons, New York.

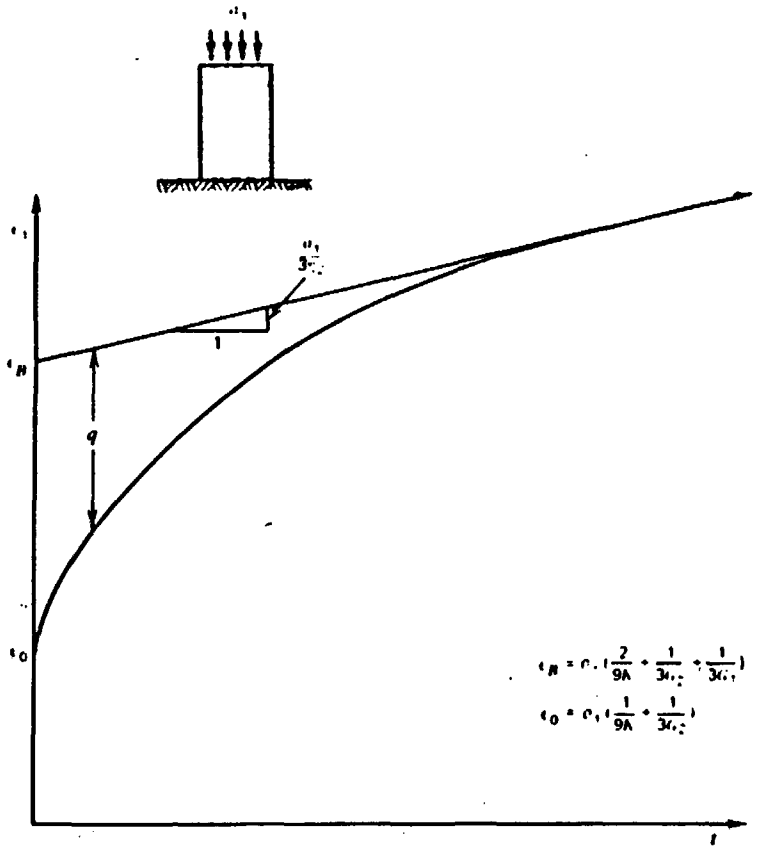

Figure 6.18 Creep in uniaxial compression of a rock that behaves as a Burgers body under deviatoric stress but an elastic body under hydrostatic compression.

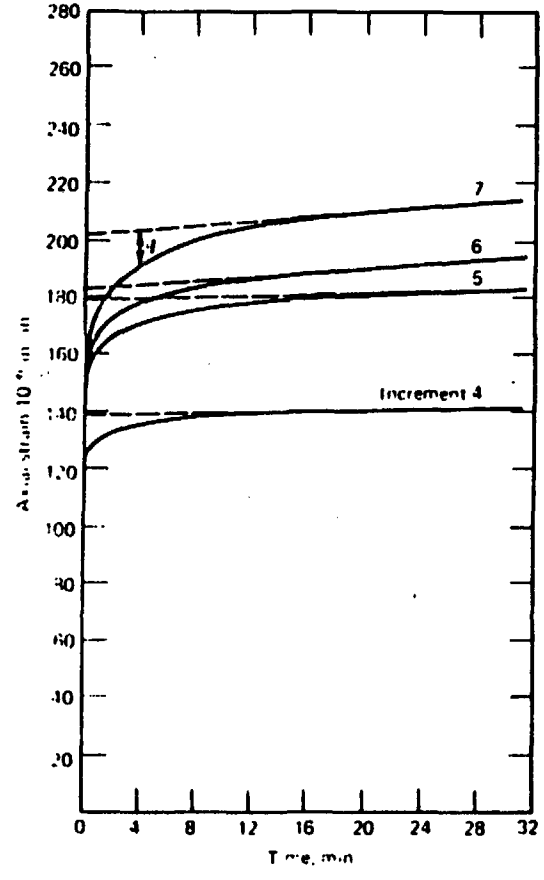

Figure 6.19 Creep of Indiana limestone in unconfined compression. [Data from Hardy, Kim, Stefanko, and Wang (1970).]

From: R.E. Goodman, 1980, Introduction to Rock Mechanics, John Wiley and Sons, New York.

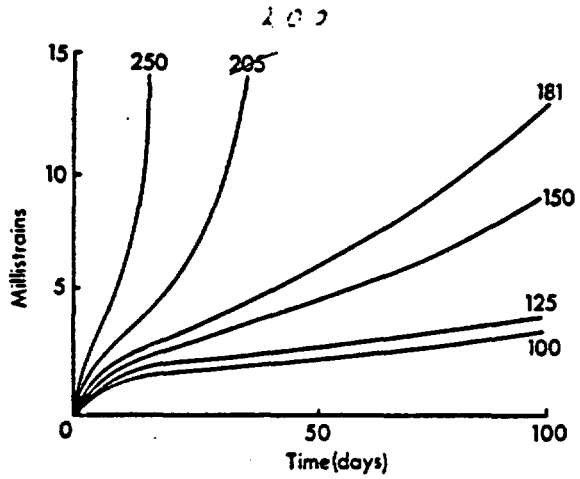

Fig. 11.1.2 Creep of alabaster in water (after Griggs. 1940). Numbers on the curves are values of the uniaxial compressive stress in bars.

From: Jaeger, J.C. and N.G.W. Cook, 1979, Fundamentals of Rock Mechanics, Third Edition, Chapman and Hall, London.

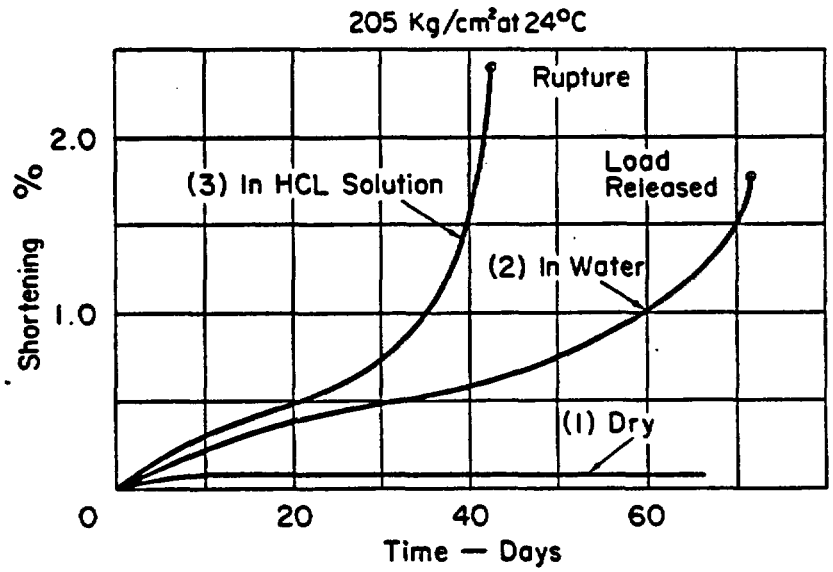

FIGURE 17 Creep of alabaster

From: R.G.K. Morrison, 1976, A Philosophy of Ground Control, Department of Mining and Metallurgical Engineering, McGill University, Montreal.

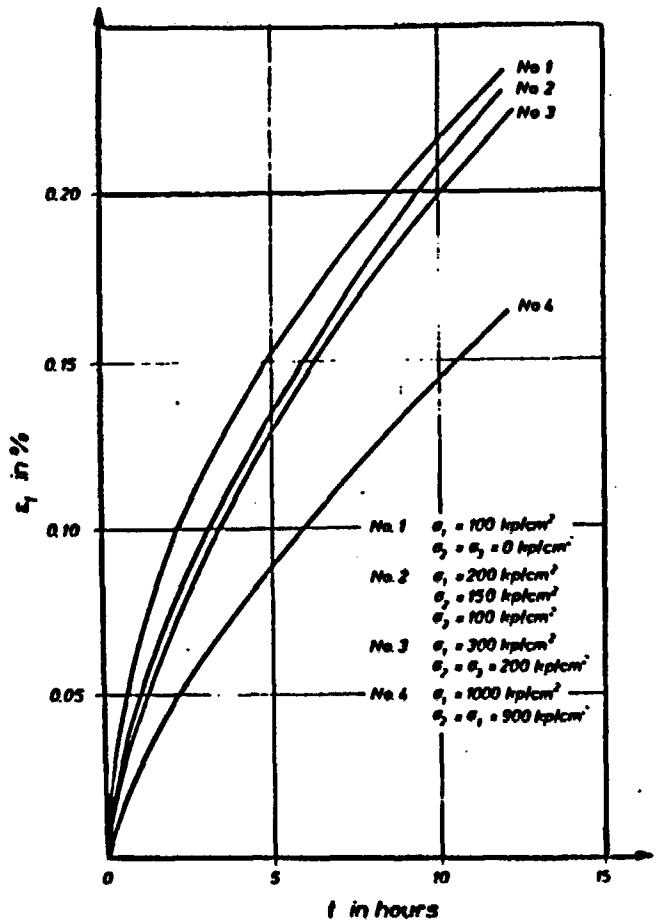

Fig. 44 : Creep curves of triaxially loaded halitic rock salt samples at constant maximum shear stresses

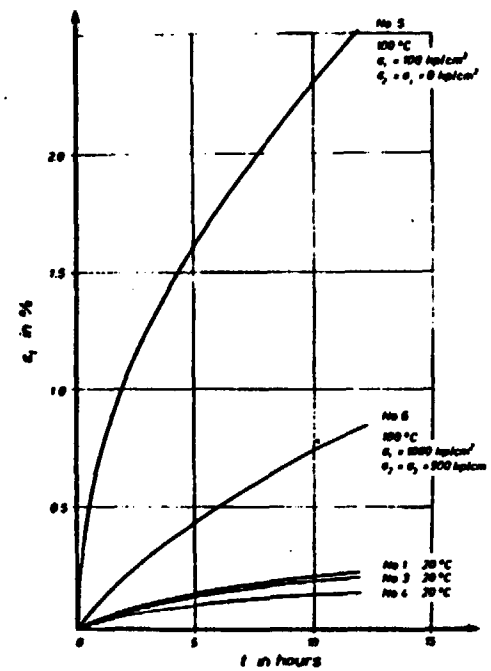

Fig. 45: Creep curves of a halitic rock salt under various triaxial loadings and test temperatures

From: W. Dreyer, 1972, The Science of Rock Mechanics, Trans Tech Publications, Clausthal-Zellerfeld.

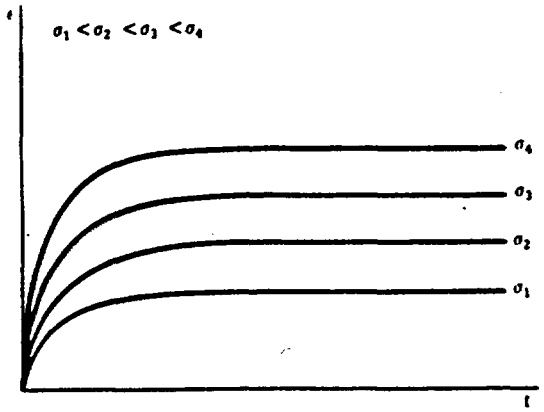

Figure 1.24. Strain-time relationships for a Kelvin material.

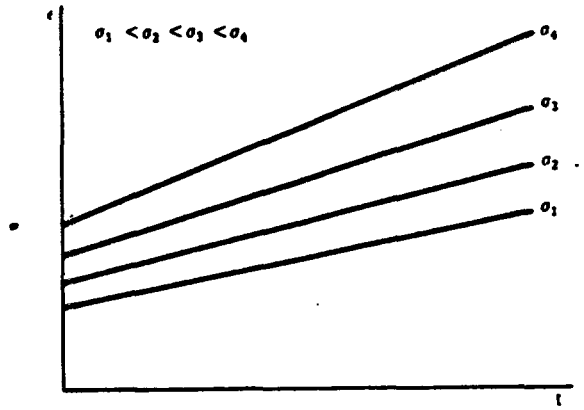

Figure 1.25. Strain-time relationships for a Maxwell material.

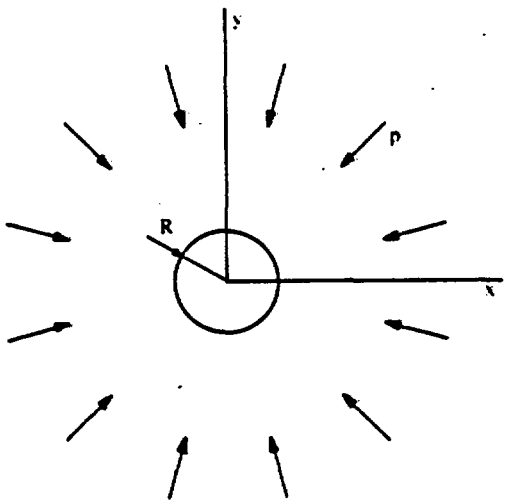

Figure 1.26. Uniformly stressed plate with a circular hole.

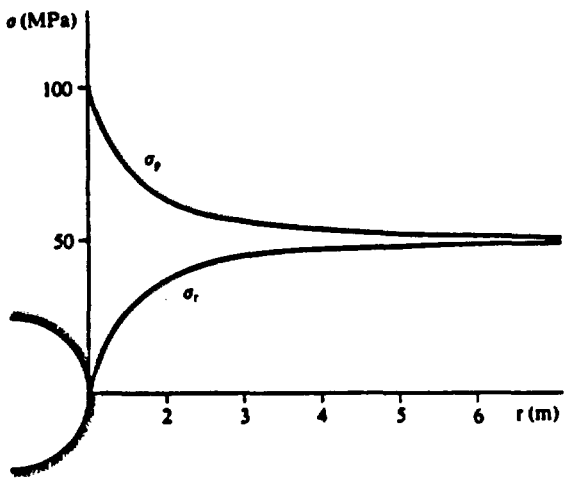

Figure 1.27. Distribution of stresses around a circular hole in a uniformly stressed plate.

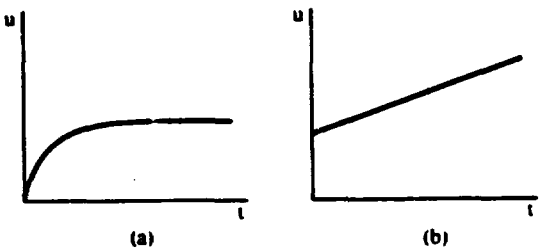

Figure 1.29. Radial displacement of a circular hole in (*a*) Kelvin and (*b*) Maxwell materials.

From: Budavari, S., 1983, Fundamental Principles of Solid Mechanics, Ch. 1 in Rock Mechanics in Mining Practice, S. Budavari, Editor, The South African Institute of Mining and Metallurgy, Johannesburg.

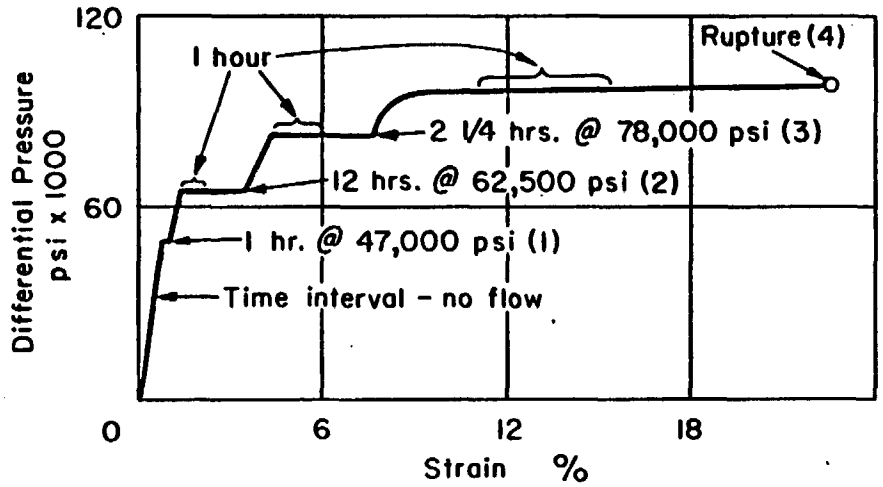

FIGURE 18 The effect of time on the flow of Solenhofen limestone, confining pressure of 10,000 atmospheres

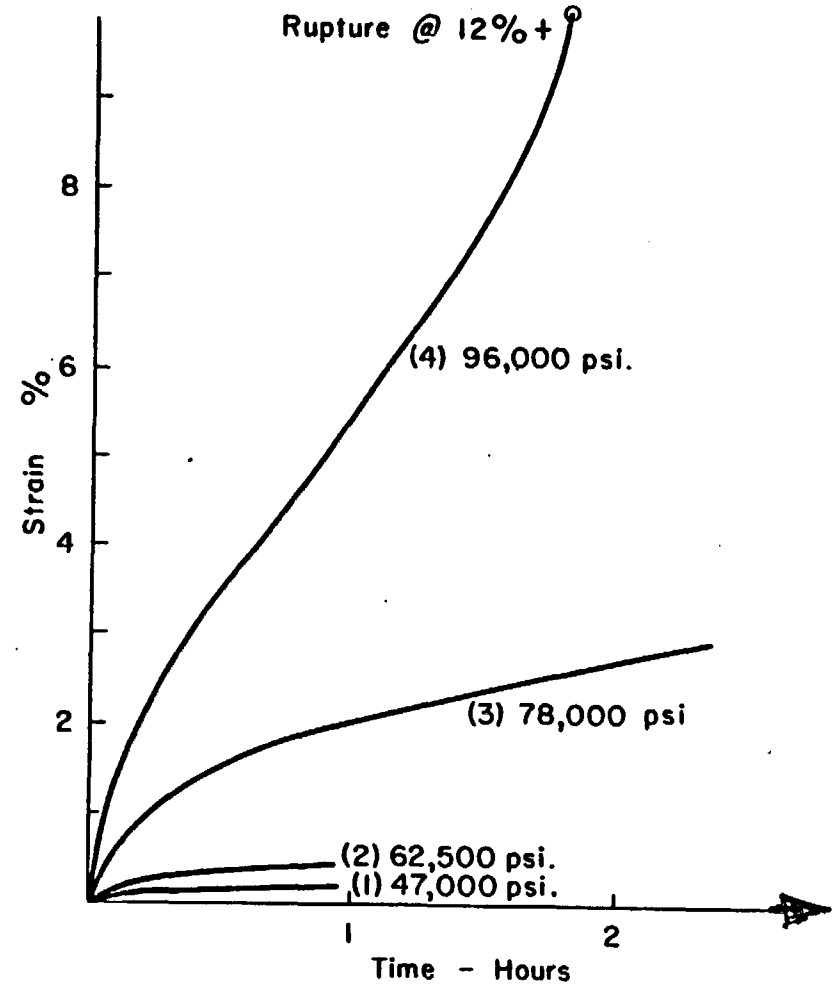

FIGURE 19 Analyses of time strain shown in Figure 18

From: Morrison, R.G.K., 1976, A Philosophy of Ground Control, Department of Mining and Metallurgical Engineering, McGill University, Montreal.

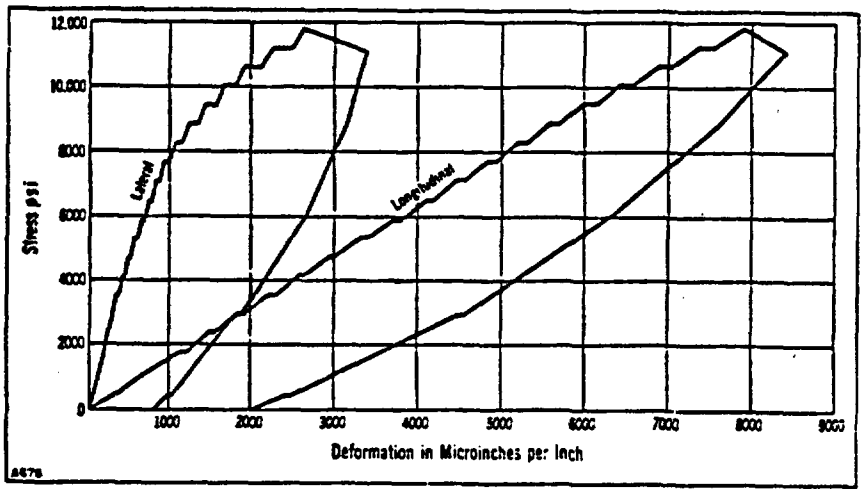

FIGURE 8 Stress-strain characteristics of a coal-measure shale: load applied in increments at 10-minute intervals (*After D. W. Phillips*[12]).

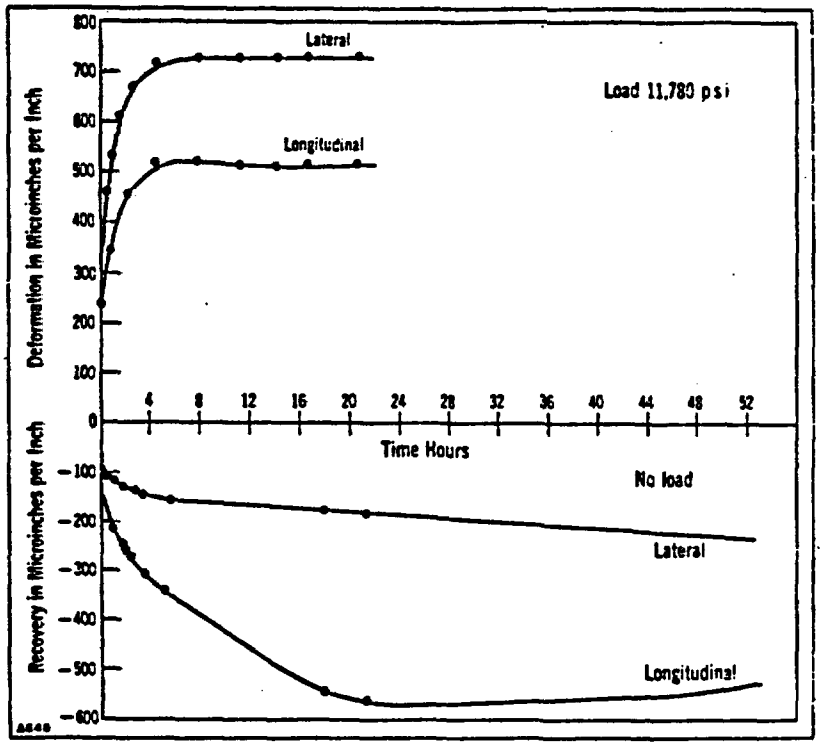

FIGURE 9 Analysis of time-strain shown in Figure 8 at full load (11,780) and upon removal of load, showing time recovery (*After D. W. Phillips*[12]).

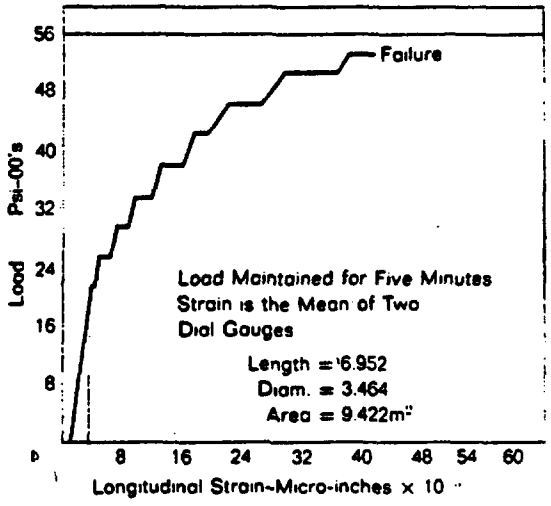

FIGURE 11
Rock Salt, Saskatchewan

From: Morrison, R.G.K., 1976, A Philosophy of Ground Control, Department of Mining and Metallurgical Engineering, McGill University, Montreal.

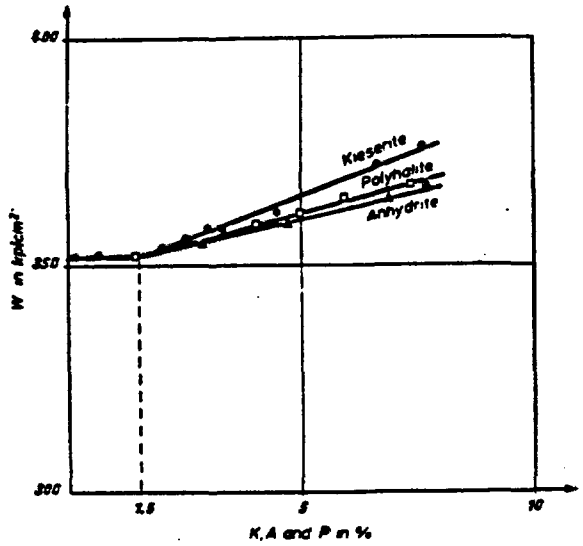

Fig. 4 : Cubical compressive strength as function of the secondary mineral content of a halitic rock salt.

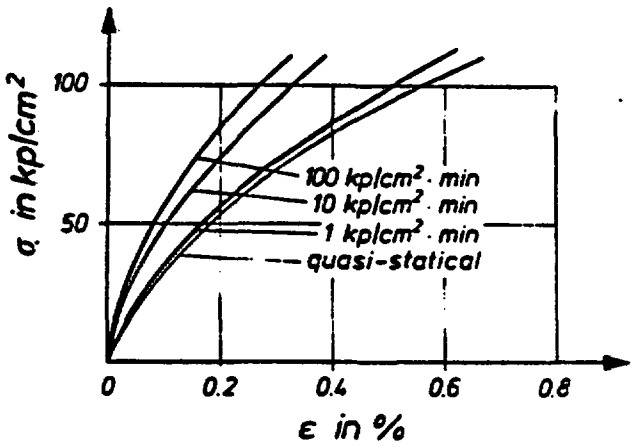

Fig. 16 : Stress - strain curves of older rock salts at various rates of loading

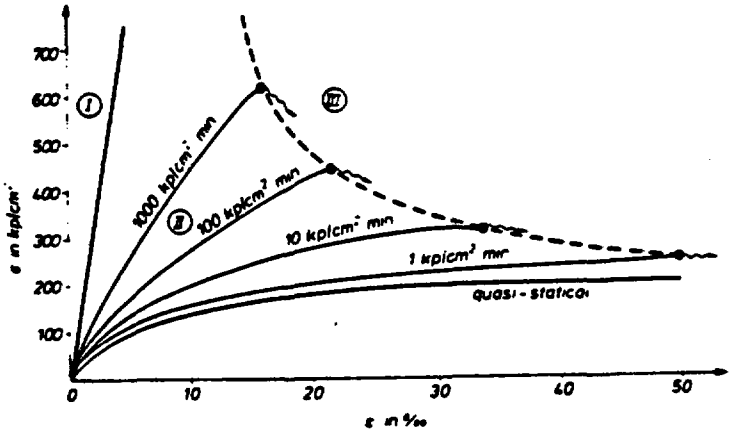

Fig. 17 : Fracture curve of a halitic rock salt under uniaxial loading

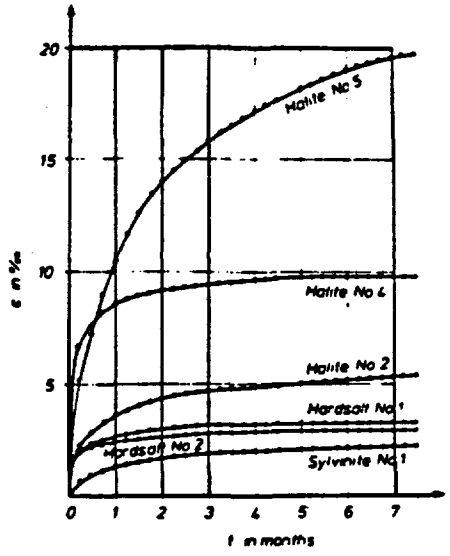

Fig. 33 : Creep curves of various rock salts under constant axial stress and test temperature

From: W. Dreyer, 1972, The Science of Rock Mechanics, Trans Tech Publications, Clausthal-Zellerfeld.

ANNEX

Constitutive laws and material parameters for rock salt (literature)

1. Transient creep ("primary creep")

1.1 Empirical laws

$\varepsilon = K \cdot \vartheta^{\alpha} \cdot \sigma^{\beta} \cdot t^{\gamma}$	potential law (1,2,3,4, 5,6,7)
$\varepsilon = A(\sigma,\vartheta) \ln (1 + \alpha t)$	logarithmic law (8,9)
$\varepsilon = B(\sigma,\vartheta) \cdot [1 - e^{-bt}]$	exponential law (10,11)
$\frac{1}{\varepsilon} = C(\vartheta) \sigma^{\beta} \cdot \varepsilon^{-\mu}$	strain hardening (12,13, 14)

1.2 Rheological laws (ϑ = const.)

$\varepsilon = \frac{\sigma}{E} (1 - e^{-\frac{E}{\eta} t})$	Kelvin-body (15)
$\varepsilon = \frac{\sigma}{E_0} + \frac{\sigma}{E} (1 - e^{-\frac{E}{\eta} t})$	Nakamura-body (16)
$\varepsilon = \sigma \cdot \sum_{i=1}^{n} \frac{1}{E_i} (1 - e^{-\frac{E_i}{\eta_i} t})$	extended Kelvin-body (17)

1.3 Structural laws (dislocation-theory)

$\varepsilon = K \cdot \sigma^{\beta} \cdot t^{\gamma} \cdot e^{-\frac{Q}{RT}}$	(18,19)
$\varepsilon = K \cdot \sigma^{\beta} \cdot [1 - e^{-bt}] \cdot e^{-\frac{Q}{RT}}$	(20)

The numbers in the brackets ( ) refer to the numbers of references in chapter four of this annex.

2. STATIONARY CREEP ("SECONDARY CREEP")

2.1 Empirical laws

$$\dot{\varepsilon} = A(\alpha)\,\sigma^{n} \qquad (21,22)$$

$$\dot{\varepsilon} = K\,\sigma^{n} \cdot \vartheta^{\alpha} \qquad (23,24)$$

2.2 Rheological laws (ϑ = const.)

$$\dot{\varepsilon} = \frac{1}{\eta}(\sigma - \sigma_{F})\,[\sigma > \sigma_{F}] \qquad \text{Bingham-body (25,26)}$$

$$\dot{\varepsilon} = \frac{1}{\eta}(\sigma - \sigma_{F}) + \frac{1}{E}\dot{\sigma}\,[\sigma > \sigma_{F}] \qquad \text{Schwedoff-body (27)}$$

2.3 Structural laws (dislocation-theory)

$$\dot{\varepsilon} = K \cdot \sigma^{n} \cdot e^{-\frac{Q}{RT}} \qquad \text{dislocation climb (28,29,30)}$$

$$\dot{\varepsilon} = K \cdot \left[\sin\frac{\sigma}{\alpha}\right]^{n} \cdot e^{-\frac{Q}{RT}} \qquad \text{dislocation glide (31,32)}$$

$$\dot{\varepsilon} = K_1\,\sigma^{n}\,e^{\frac{-Q1}{RT}} + K_2 e^{\frac{-Q2}{RT}} \cdot f(\sigma) \qquad \text{comb. mechanism (33,34)}$$

3. TRANSIENT AND STATIONARY CREEP

3.1 Empirical laws (ϑ, σ = const.)

$$\varepsilon = \varepsilon_0 + kt + at^{\gamma} \qquad (35)$$

$$\varepsilon = \varepsilon_0 + kt + b\ln(1+ct) \qquad (36)$$

$$\varepsilon = \varepsilon_0 + k't + d\ln\left[n+(1-n)\, e^{-\frac{\dot{\varepsilon}_s}{\alpha} t}\right] \qquad (37)$$

3.2 Rheological laws (ϑ = const.)

$$\varepsilon = \sigma \cdot \left[\frac{1}{E_0} + \frac{1}{E}\left(1-e^{-\frac{E}{\eta} t}\right) + \frac{1}{\eta_m} t\right] \qquad \text{Burgers-body.} \quad (38)$$

$$\varepsilon = \sigma \cdot \left[\frac{1}{E_0} + \frac{1}{E}\left(1-e^{-\frac{E}{\eta} t}\right)\right] + (\sigma - \sigma_F) \cdot \frac{1}{\eta_m} t \qquad \text{Schofield-ScottBlair-body} \quad (39)$$

$$\varepsilon = \sigma\left[\frac{1}{E} - \frac{1}{E}\left(1-e^{-\frac{E}{\eta} t}\right)\right] + (\sigma - \sigma_{Kr}) \cdot \sum_{i=1}^{n} \frac{1}{E_i} \cdot \left(1-e^{-\frac{E}{\eta} t}\right) + (\sigma - \sigma_F) \cdot \frac{1}{\eta_m} \cdot t$$

Schofield-ScottBlair-body, extended (40)

3.3 Structural laws (dislocation-theory)

$$\varepsilon = B \cdot e^{-\frac{Q}{RT}} \cdot \sigma^{n} \left[1-e^{-mt}\right] + A\, e^{-\frac{Q}{RT}} \cdot \sigma^{n} \cdot t \qquad (20)$$

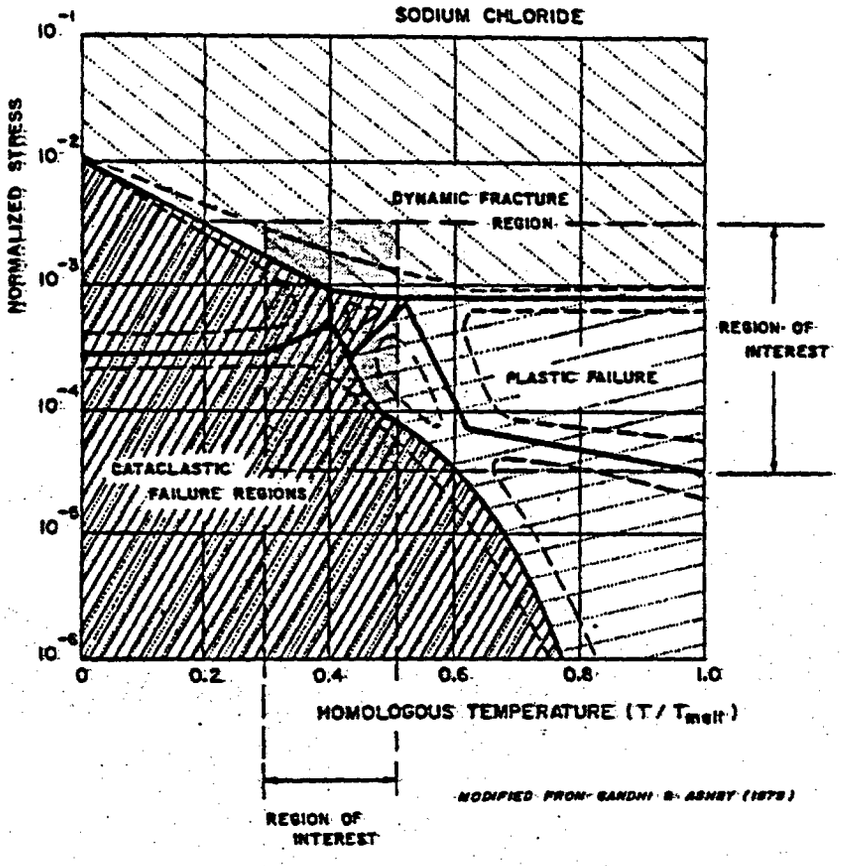

Figure 1 — Deformation Map

However, the precise transition boundaries between creep mechanisms of halite are as yet undefined by experimental observation. Most petrographic data to date are from samples subjected to constant-rate testing, and not from creep tests. Moreover, the transition between mechanisms is gradual and the stress/temperature boundaries are not distinct, but are actually zones of transition.

Despite these problems, certain transition bounds in creep can tentatively be identified. For low-confining pressures of approximately 3.5 MPa or less, and at temperatures below 75°C, plastic deformation is controlled by fracture propagation of existent defects. Failure is characteristically brittle, consisting of a distinct failure plane or zone through the sample (Hansen and Carter, 1980). At higher pressures and temperatures, between 100 and 200°C, the controlling mechanism is

of time (less than a year) can be fitted equally well to both concepts (Herrmann and Lauson, 1981). In contrast, the numerical determination of steady state values has shown to be quite consistent, regardless of the transient model employed in the combined transient and steady state expression (Herrmann, et al., 1980). This lends some credence to the existence of such a term. It is noted that the impact of this difference in response models becomes only important at long time periods.

TABLE 1

Examples of Empirical Equations for Creep of Rock Salt

Equation-Form[1]	Data Source	Test Conditions & Comments
$\varepsilon = A + Bt\exp + Ct$ $A = 1.16 \times 10^{-3}$ $B = 1.00 \times 10^{-3}$ $C = 2.90 \times 10^{-7}$	Laboratory Test, Single Crystal Size: 1.1 x 1.1 x 2.05 cm Griggs (1939)	Uniaxial Compression Tests Axial Load: 0.61 MPa Temperature: 23°C Duration: 1000 Hours
$\varepsilon = A + Bt^n$ Data #1: $A = 7.0 \times 10^{-4}$ $B = 1.30 \times 10^{-3}$ $n = 0.305$ Data #2: $A = 8.20 \times 10^{-3}$ $B = 6.0 \times 10^{-4}$ $n = 0.642$ $n = 1.5 - 0.011(\theta - 273)$ $B = 1.2 + 0.30(\theta - 273)$	Laboratory Test, Artificial Salt Diameter: 3.18 cm Length: 6.13 cm Lo Conte (1965)	Triaxial Compression Tests #1 #2 Axial Load: 6.9 MPa 107 MPa Lateral Load: 0.0 MPa 100 MPa Temperature: 23°C 100.5°C Duration: 100 Hours 100-150 Hours Equation for n and B at 10.2 MPa Equations Derived from Figures. Maximum Test Temperature: 250°C
$\varepsilon = \sigma^n t^p \theta^q$ $A = 1.19 \times 10^{-31}$ $n = 9.5$ $m = 0.3$ $p = 3.0$	Laboratory Test, Halite Diameter (Inner): 10.0 cm Length: 7.6 cm (Dumbell Shaped Samples) Lomnick (1971)	Uniaxial Compression Test with Steel Collars Axial Load: 13.8 - 68.9 MPa Temperature: 22.5 - 200°C Duration: 600 - 1000 Hours
$\varepsilon = A\sigma^n t^p$ $A = 2.13 \times 10^{-6}$ $n = 0.38$ $p = 2.02$	Laboratory Test, Halite Diameter: 5.08 cm Length: 10.2 cm Hansen (1977)	Triaxial Compression Tests Axial Load: 10.3 - 41.4 MPa Lateral Load: 0 - 10.3 MPa Temperature: 22°C (?) Duration: 120 - 250 Hours
$\dot{\varepsilon} = A\exp(-B - Ct)$ $A = 6.2 \times 10^{-1}$ $B = 3.0$ $C = 4.2 \times 10^{-2}$	In-Situ Monitoring Depth: 215 m Sorets & Gloyna (1960)	Duration: 1 Year (8760 Hours) Time after Mining: 5/10 Years
$\varepsilon = A + Bt + C(1 - \exp(Dt))$ $A = 4.30 \times 10^{-2}$ $B = 2.15 \times 10^{-6}$ $C = 2.35 \times 10^{-2}$ $D = 4.50 \times 10^{-3}$	Laboratory Test, Halite Diameter (Inner): 10.0 cm Length: 7.6 cm (Dumbell Shaped Samples) Ehern (1965)	Uniaxial Compression Tests with Steel Collars Axial Load: 13.8 - 68.9 MPa Temperature: 23°C (?) Duration: 1000 Hours (Maximum)
$\dot{\varepsilon} = \sigma^n$ $n = N/A$ $p = 2.4$ to 3.3		
$\varepsilon = \left(\frac{B\sigma^n}{\theta + C\sigma^p}\right) + D$ $A = 5.1 \times 10^{-3}$ $B = 5.3 \times 10^{-6}$ $C = 1.4 \times 10^{-3}$ $D = 1.2 \times 10^{-2}$	Laboratory Test, Halite Size: 4 x 4 x 10 cm Dreyer (1972)	Uniaxial Compression Test Axial Load: 620Kp/cm^2 Temperature: 10°C Duration: 3600 Hours
$\varepsilon = A\sigma^n t^p$ $A = 2.22 \times 10^{-7}$ $n = 0.382$ $p = 3.26$	Laboratory Test, Halite Size N/A Mair & Gaere (1968)	Uniaxial Triaxial Extension Test Axial Load: 10.3 - 27.6 MPa Temperature: N/A Duration: 10 - 1000 Hours
$\dot{\varepsilon} = A\theta^p$ $A = 4.28 \times 10^{-3}$ $p = 2.7$	In-Situ Monitoring Depth: Varied Hadley (1967)	Duration: N/A Time after Mining: Varied (3 - 40 Years)
$\dot{\varepsilon} = A\theta^p$ $A = 1.78 \times 10^{-13}$ $p = 5.24$	Laboratory Test, Halite Diameter: 10.2 cm Length: 20.3 - 130.5 cm Thompson & Dipperberger (1964)	Uniaxial Compression Test Axial Load: 9.6 - 16.5 MPa Temperature: 32°C Duration: 16.7 Hours
$\dot{\varepsilon} = A\exp(\theta + Bt)$ $A = 0.56 \times 10^{-3}$ $B = 2.13 \times 10^{-4}$	In-Situ Monitoring Depth: 520 m Mair & Cameron (1966)	Duration: 2.9 Years (25,200 Hours) Time after Mining: 0.6 Years
$\dot{\varepsilon} = A\exp(-Bt)$ $A = 6.03$ $B = 7.3 \times 10^{-6}$	In-Situ Monitoring Depth: 215 m Reynolds & Gloyna (1961)	Duration: 2 Years (17,500 Hours) Time after Mining: 5/10 Years

TABLE 1 (cont'd)

Examples of Empirical Equations for Creep of Rock Salt

Equation-Form[1]	Data Source	Test Conditions & Comments
$\dot{\epsilon}_1 = A\,\theta^{\alpha}\,t^{m}\,S^{p}$ Eq. (1) $A = 4.88 \times 10^{-35}$ $\alpha = 11.4$ $m = 0.48$ $p = 3.3$	Laboratory Tests, Halite (New Mexico & Louisiana) Diameter: 50 cm Hansen and Carter (1980)	Triaxial Compression Tests Axial Load: 5.5 - 41.4 MPa Lateral Load: σ_L - 20.7 MPa Temperature: 20° - 200°C Analyses of 86 transient data curves. Results from differing functions differ only slightly. Equations represent different expressions of the data base ($\dot{\epsilon}_1$) in transient creep, ($\dot{\epsilon}_2$) in secondary creep.
$\dot{\epsilon}_2 = A\,t^{m}\,S^{p}\,\exp\left(\frac{-Q}{RT}\right)$ Eq. (2) $A = 6.48 \times 10^{-1}$ $m = 0.5$ $p = 3.5$ $Q = 36.0$ KJ/mole		
$\dot{\epsilon}_3 = A\,\exp\left(\frac{-Q}{RT}\right)\,S^{p}$ Eq. (3) $A = 1.48 \times 10^{-2}$ $Q = 45.2$ KJ/mole $p = 3.3$		
$\dot{\epsilon}_3 = A\,\exp\left(\frac{-Q}{RT}\right)\,S^{p}$ $A = 7.5 \times 10^{-3}$ $Q = 54.24$ KJ/mole $p = 5.0$	Laboratory Tests, Halite Diameter: 10.0 cm Length: 22.0 cm Langer & Mellmer (1979)	Triaxial Compression Tests Axial Load: N/A Temperature: 25°, 100, 150, 200, 300°C
$\dot{\epsilon}_3 = A\left(\frac{\sigma}{G}\right)^{p}\,\exp\left(\frac{-Q}{RT}\right)$ $A = 9.6/29.5 \times 10^{-12}$ $G = 12.4$ GPa $p = 4.90$ $Q = 50.2$ KJ/mole $R = 8.319$ J/mole - °K	Laboratory Tests, Halite (Jaw-Matica) Diameter: 5.0 and 10.0 cm Hornemann et al. (1980)	Axial Load: 7 - 41 MPa Temperature: 22, 70, 100, 200°C Duration: N/A Confining Pressure: 0 - 21 MPa Analyses of several groups of data from 2 different laboratories. A parameter varied for differing salt sections. Values from exponential curve-fit; results from logarithmic fit differ only slightly.
$\dot{\epsilon}_3 = A\,S^{p}$ $A = 3.67 \times 10^{-12}$ $p = 5.5$	In-Situ Monitoring Depth: 1250 m. Pritz & Hampelers (1981)	Borehole-Convergence Results, Asse-Mine (West Germany) Analyses based on Finite Element Modeling

Note: (1) Time (t) is in hours, Temperature (θ) is in °Kelvin, and Deviatoric Stress (S) is in MPa.
(2) Equation values have been changed to the above units, when required, from original source.

where predictions from the two concepts diverge significantly.

The final observation is that none of the present creep laws considers any influence of the previous specimen stress/strain history. However, definite memory aspects of creep have been observed in metals (Krempl, 1974), which would suggest the possible existence of memory in materials such as halite. It is postulated, therefore, that a rigorous description of rock salt response should incorporate the probable role of load deformation history. All of the models discussed previously are deficient in this respect.

THEORETICAL FORMULATION

Problem Definition

The purpose of the present theoretical discussion is to construct a simple model to evaluate several possible aspects of salt creep. The model will not be a complete constitutive formulation, but rather a response model to simulate the time-dependent behavior of rock salt under constant stress. It is of importance to note that all of the empirical creep equations listed in Table 1 are also response models and that development of a general constitutive model utilizing these models

Here, the case of the plain strain state is to be investigated. The cavern is assumed to be filled with brine, with a cavern head pressure of $p_{i,WH} = 0$ MPa. At a depth of 1000 m this results in a cavern internal pressure of $p_i \approx 12$ MPa. At this depth the rock pressure is about $p_o \approx -22$ MPa. The other rock characteristics can be obtained from Figure 25.

The time-dependant stresses, strains and displacements are calculated for the material laws given in the equations (6) to (10). The UTROEFV program developed out of the finite-element-method of the Lehrgebiet für Unterirdisches Bauen, LUB [1979], is drawn on for this. The elastic stress state resulting from the load case "brine - filled cavern" is taken as the initial stress state for the viscous calculations.

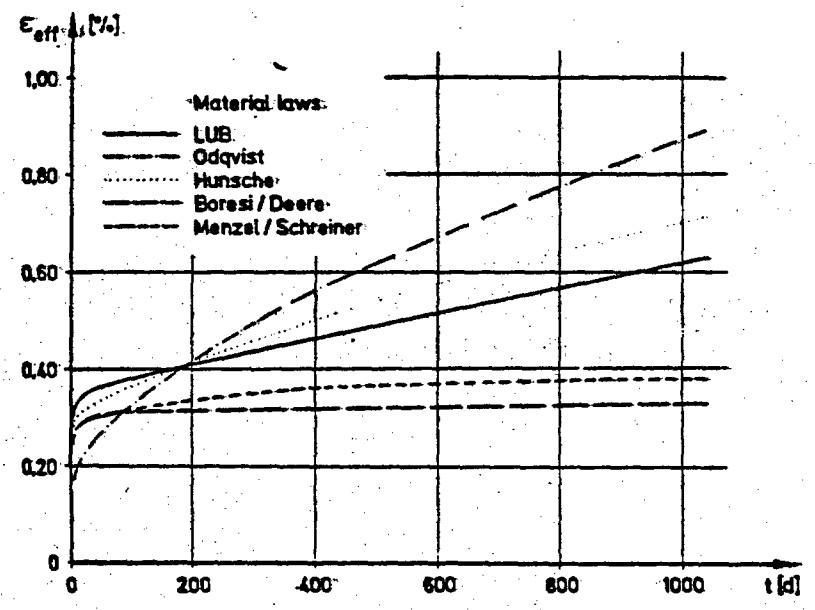

Figure 26 Effective creep strains predicted with different creep laws

Figure 26 shows above all the effective strains in dependance on the time over a period of 1000 days. The effective strains result according to equation (11a) from the individual viscous strain components as

$$\varepsilon_{eff} = \sqrt{\frac{2}{3}\left(\varepsilon_r^2 + \varepsilon_z^2 + \varepsilon_\varphi^2 + \frac{1}{2}\gamma_{rz}^2\right)} \qquad (11\,a)$$

In view of the rational symmetry and the plain strain

$$\varepsilon_z = \gamma_{rz} = 0 \qquad (11\,b)$$

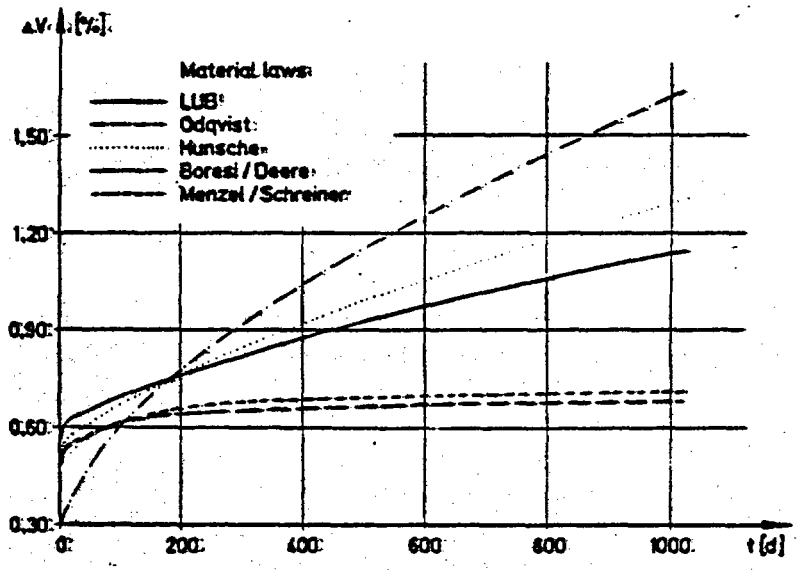

Figure 29 Volume creep convergence predicted with different creep laws

ΔV = o.70 % after 1000 days and an only extremely slight increase. After 500 days the convergence here is already ΔV = 0.67 % and therewith more than 95 % of the final value. The convergences prognosticated with the other material laws lie between ΔV = 1.13 % for the LUB material law and ΔV = 1.61 % for the Odqvist material law and reveal an only slightly declining rate of convergence. The comparative values after 500 days amount to only ΔV = 0.93 % respectively, 1.15 %. From this the increase which can also be expected for longer periods can be seen.

SUMMARY AND OUTLOOK

This paper is concerned with some aspects of laboratory tests with rock salt and with salt cavern design. First of all, a general review is given of the work to be carried out within the scope of rock mechanical investigations, for the design and preparations of cavern plants in rock salt and possible design criteria for the assessment of theoretical results. The presentation and discussion then follows of results from own laboratory tests on the strength and deformation behaviour of rock salt material from various locations. Finally, basing on the results of uniaxial creep tests, some problems are discussed which are connected with the formulation of viscous material laws and the data obtained with them which affect creep behaviour. In particular, a comparative investigation into the extrapolation of laboratory timings is carried out, which lie in the range of weeks and a few months, with reference to relevant periods of years for cavern plants.

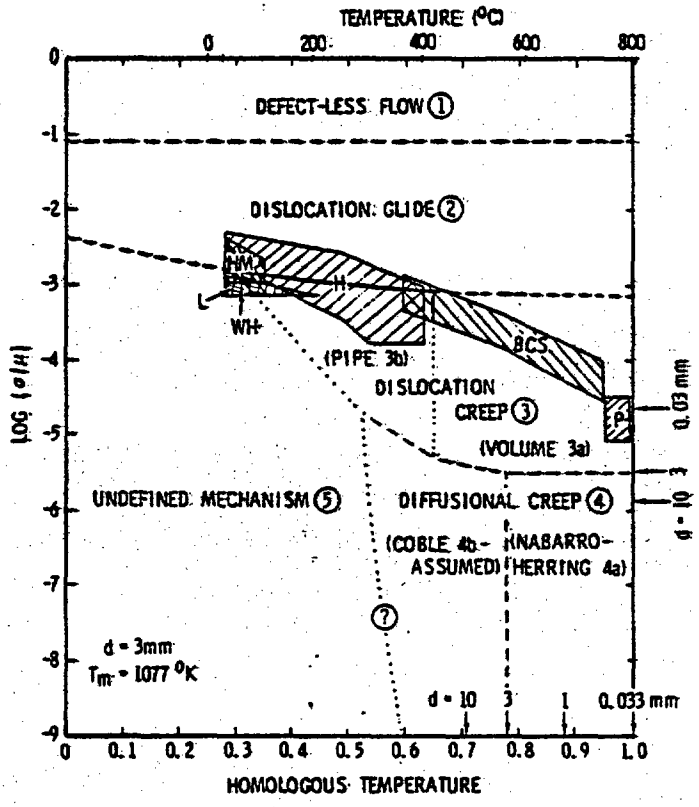

Figure 1. — Preliminary deformation-mechanism map with an overlay of the envelopes of experimental investigations, after Munson [2]. Grain size is 3 mm. Experimental ranges are from Poirier (P) [8], Burke, et al, (BCS) [9], Heard (H) [10], Hansen and Mellegard (HM) [11], Le Comte (L) [12], and Wawersik and Hannum (WH) [13].

at which this regime begins has been derived from atomic binding considerations. For the onset of defectless flow in salt, the dimensionless deviatoric stress, σ/μ, is equal to 0.086 at absolute zero temperature ($T/T_m = 0$). Clearly, this stress regime is of little engineering importance, since stresses of such a magnitude will never be reached in practical applications.

Dislocation Glide—Regime 2

Salt, which crystallizes in the cubic system, has several slip systems that permit it to deform readily by dislocation motion.

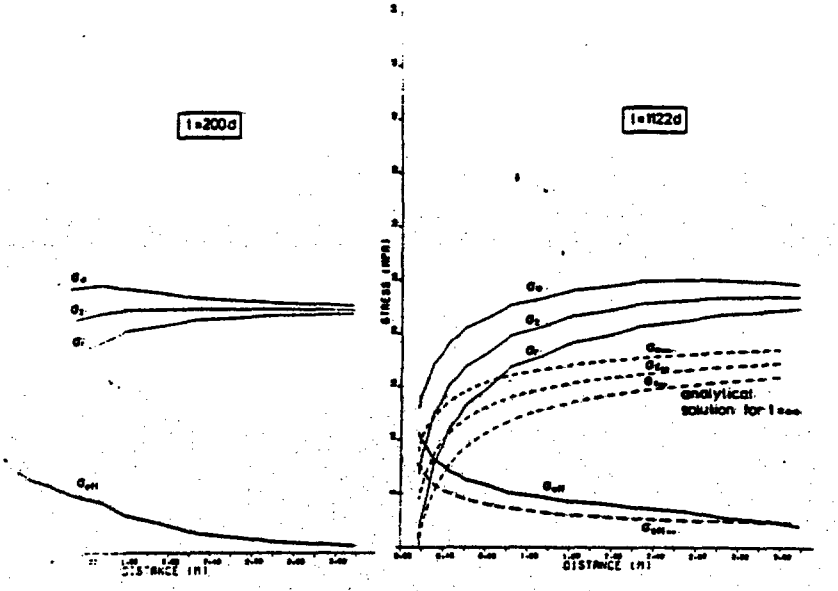

Fig. 4: Continued

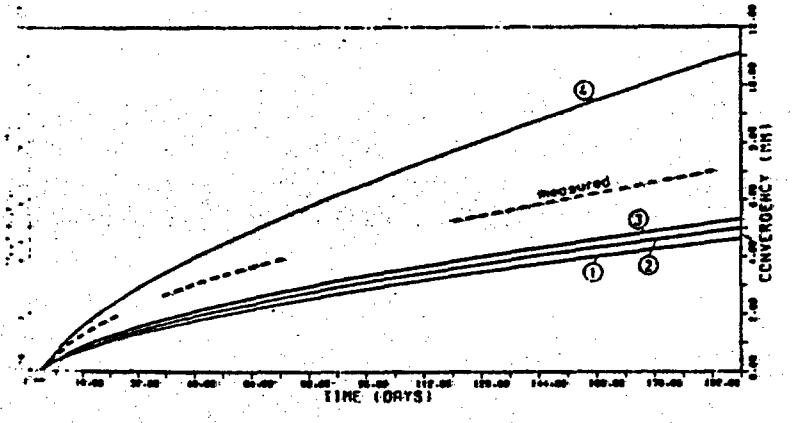

Fig. 5: Borehole convergence, comparison with measured values

Salt "Creep" (Behavior) Issues

In Situ vs. Lab

- loading sequence (stress path)
- scale
- salt composition

In Situ variability - representativeness

Geometry: hole closure prediction

(constitutive model problems?)
(parameter problems?)
(boundary condition problems?)

Inhomogeneity modeling

Constitutive modeling

- formulations
- experimental evaluation

Deformation - Mechanism Maps

Field test interpretation

constitutive law parameters?
empirical prediction parameters?

How much understanding is required to assess repository performance?

Rock Strength

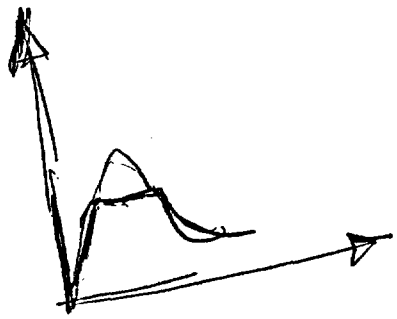

- Definition of failure
- Effective stress
  applicable in low permeability rocks?
- Pore fluid influence
- Influence of intermediate principal stress
- Influence of loading rate
- Influence of specimen size
- Anisotropic rock strength
- Rock with multiple discontinuities
- Strength of "granulated" marble

Pillar Strength

$$S = S_1 v^a (w_p/h)^b = S_2 h^\alpha w_p^\beta$$

S: pillar strength

S_1, S_2: rock strength

v, w_p, h: pillar volume, width, height

a, b, α, β: empirical parameters

Example: $S = S_1 v^{-0.118} (w_p/h)^{0.833}$

$$S_p = S_s (v_p/v_s)^{-0.118} [(w_p/h_p)/(w_s/h_s)]^{0.833}$$

(Hardy and Agapito, 1977, quoted by Brady and Brown)

Brady, B.H.G. and E.T. Brown, 1985, Rock Mechanics for Underground Mining, George Allen & Unwin, London.

Holland-Gaddy: $S_p = (S_s \sqrt{D} \sqrt{L})/T$ (coal pillars)

S_p, S_s: pillar, sample strength

D, L: (cubic) sample, (shortest) pillar length

T: pillar (seam) thickness

Holland, C.T., 1973, Mine Pillar Design, Section 13.8 of SME Mining Engineering Handbook, Society of Mining Engineers of AIME, New York.

Fairhurst: $S = k\, w^\alpha H^\beta$

α: 0.4-0.5 β: -1 to 0

Fairhurst, C., 1973, Laboratory Testing of Rock and Its Relevance to Mine Design, Section 13.3, SME Mining Engineering Handbook, Society of Mining Engineers of AIME, New York.

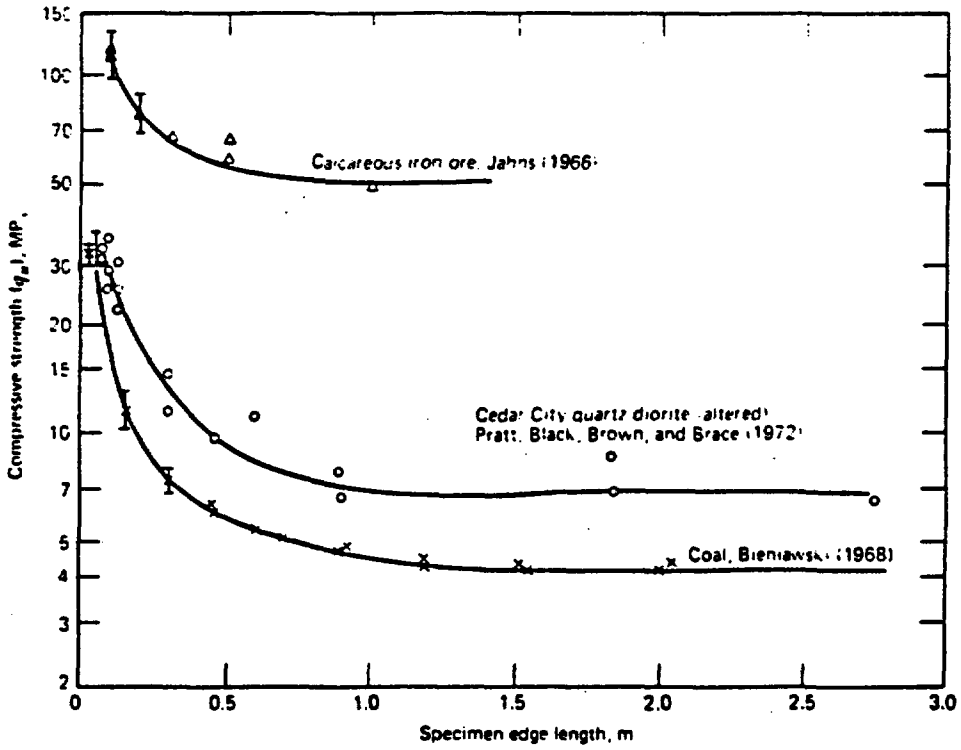

Figure 3.21 Effect of specimen size on unconfined compressive strength. [After Bieniawski and Van Heerden (1975).]

From: R.E. Goodman, 1980, Introduction to Rock Mechanics, John Wiley and Sons, New York.

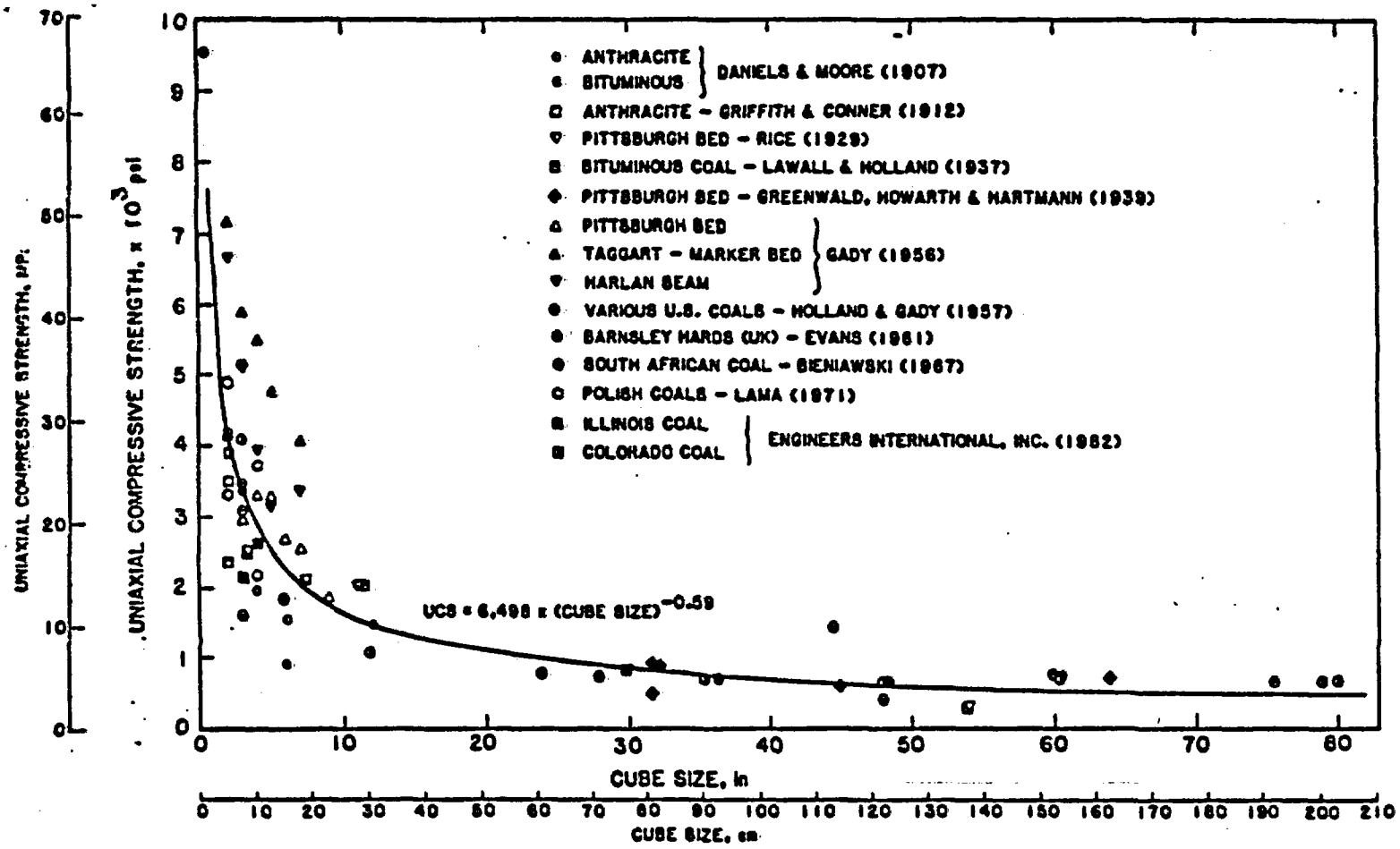

Figure 5.14. Effect of size on compressive strength of coal (after Singh, 1981).

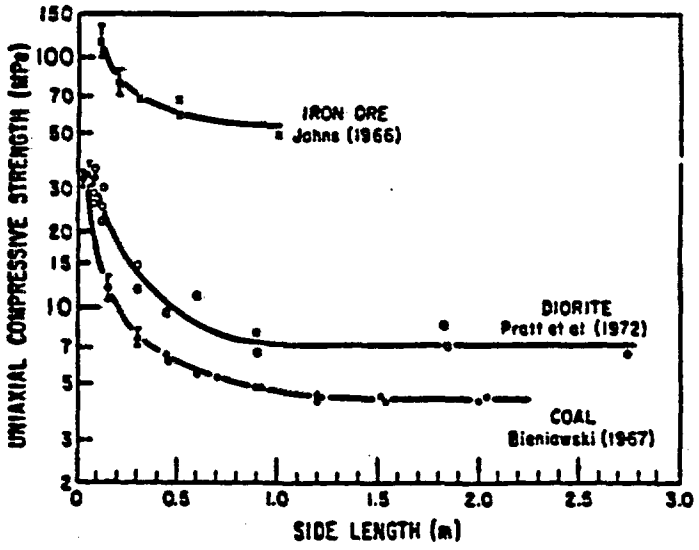

Figure 5.15. Variation of rock strength with specimen size.

From: Bieniawski, Z.T., 1984, Rock Mechanics Design in Mining and Tunneling, A.A. Balkema, Rotterdam.

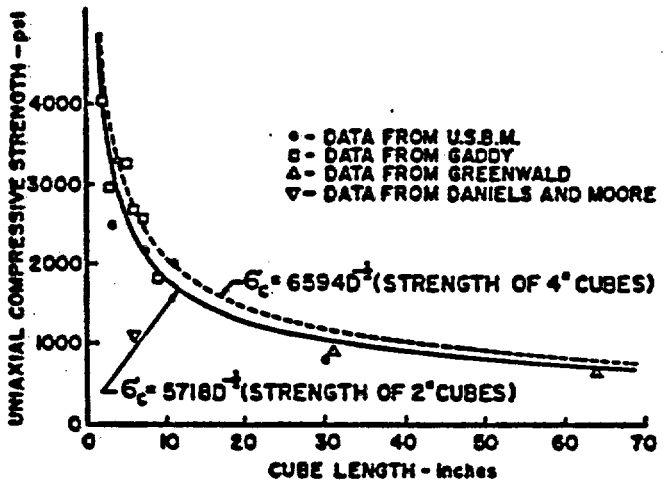

Figure 9.5. Compressive strength as a function of cube size for Pittsburgh coal (after Hustrulid, 1975).

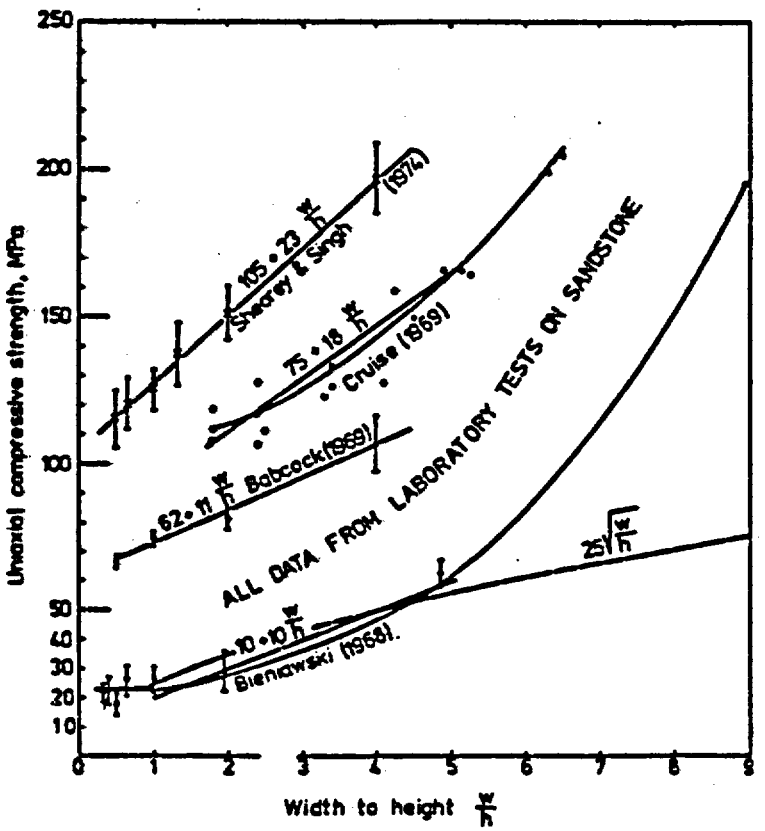

Figure 9.6. Effect of specimen width-to-height ratio on the strength of sandstone.

From: Bieniawski, Z.T., 1984, Rock Mechanics Design in Mining and Tunneling, A.A. Balkema, Rotterdam.

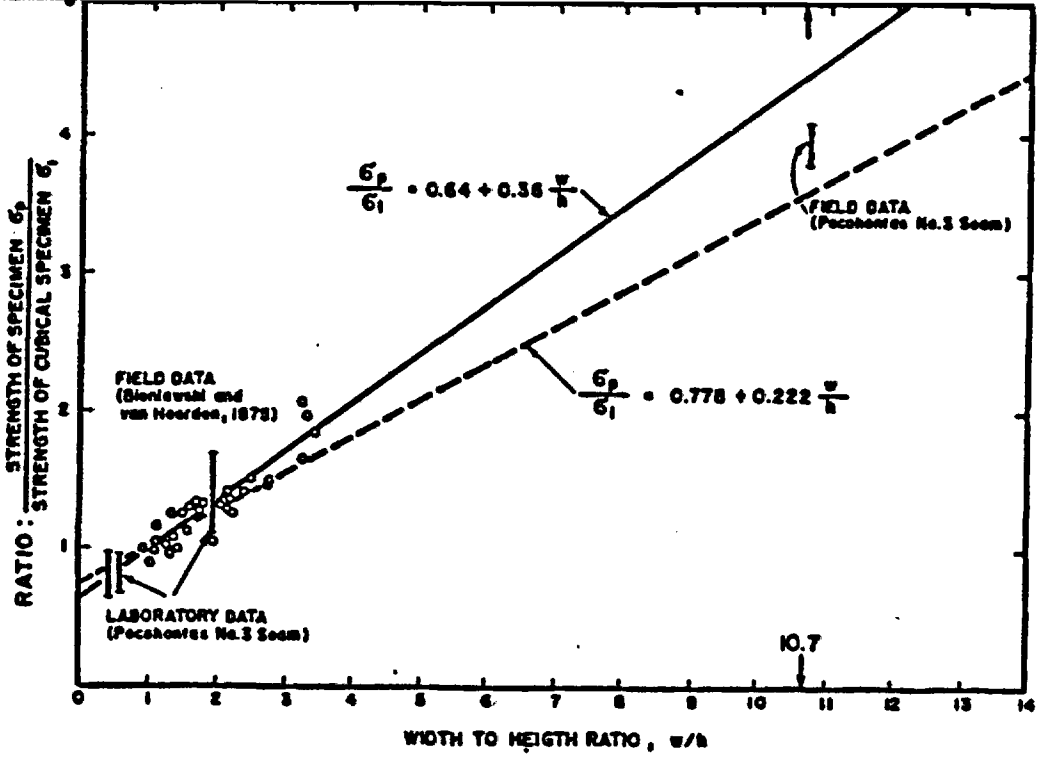

Figure 9.8. The effect of specimen width-to-height ratio on strength of coal (after Wang et al. 1977, and Bieniawski and van Heerden, 1975).

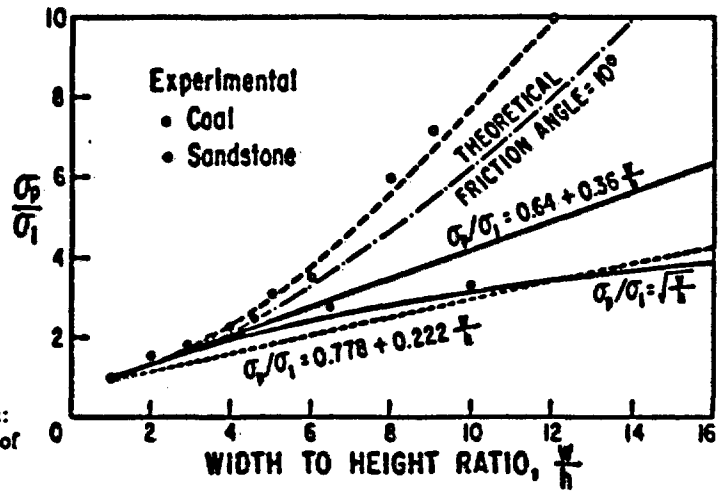

Figure 9.9. Pittsburgh seam: Strength ratio vs. w/h ratio of pillars.

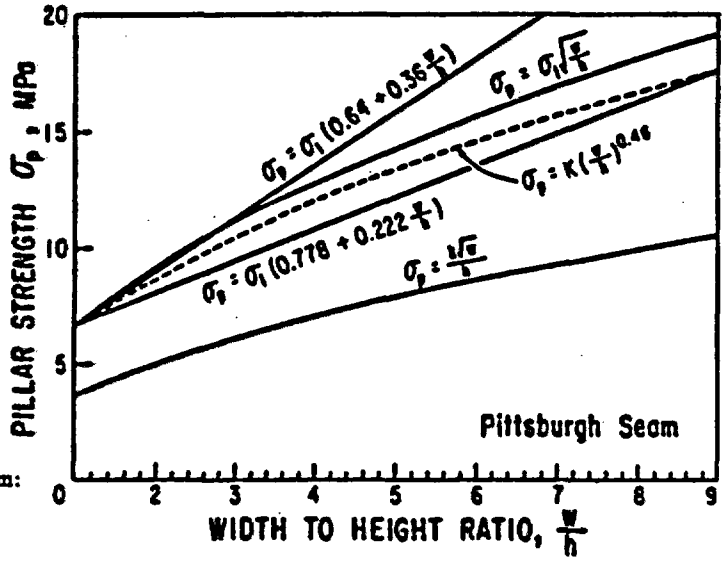

Figure 9.10. Pittsburgh seam: Strength vs. pillar width to height ratio.

From: Bieniawski, Z.T., 1984, Rock Mechanics Design in Mining and Tunneling, A.A. Balkema, Rotterdam.

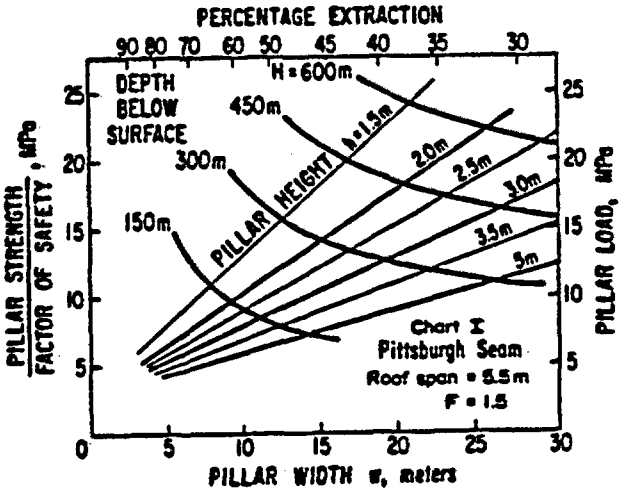

Figure 9.13. Design chart for Pittsburgh seam showing pillar strength versus pillar width for different pillar heights and different depths (roof span 5.5 m, factor of safety $f = 1.5$).

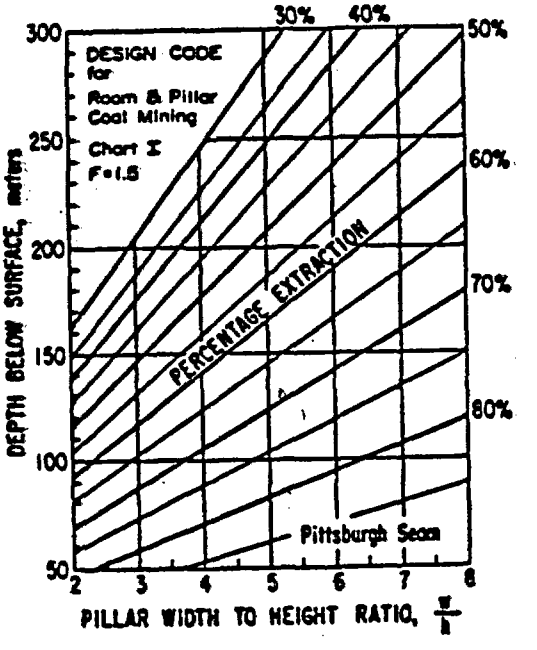

Figure 9.14. Design chart for room and pillar coal mining in the Pittsburgh seam showing depth below surface vs w/h ratio for different percentage of coal extraction and factor of safety $f = 1.5$.

From: Bieniawski, Z.T., 1984, Rock Mechanics Design in Mining and Tunneling, A.A. Balkema, Rotterdam.

Rock Mass Strength

Hoek E. and E.T. Brown, 1982, Underground Excavations in Rock, The Institution of Mining and Metallurgy, London. Chapter 6.

Rock failure criterion for underground opening design:

- cover full range of stress conditions
- account for discontinuities
- allow for projection to full-scale rock mass

Proposed empirical criterion:

$$\sigma_1 = \sigma_3 + \sqrt{m\sigma_c\sigma_3 + s\sigma_c^2}$$

σ_1, σ_3: major and minor principal stresses at failure

σ_c: uniaxial compressive strength

m, s: semi-empirical constants

Mohr envelope:

$$\sigma = \sigma_3 + \frac{\tau_m^2}{\tau_m + m\sigma_c/8}$$

$$\tau = (\sigma - \sigma_3)\sqrt{1 + \frac{m\sigma_c}{4\tau_m}}$$

where $\tau_m = (\sigma_1 - \sigma_3)/2$

Table 5.8. Approximate relationship between rock mass quality and constants (after Hoek and Brown, 1980)

Empirical failure criterion $\sigma_1 = \sigma_3 + \sqrt{m\sigma_c\sigma_3 + s\sigma_c^2}$ σ_1 = major principal stress; σ_3 = minor principal stress; σ_c = uniaxial compressive strength of intact rock, and m, s = empirical constants	Carbonate rocks with well developed crystal cleavage Dolomite, limestone and marble	Lithified argillaceous rocks Mudstone, siltstone, shale and slate (normal to cleavage)	Arenaceous rocks with strong crystals and poorly developed crystal cleavage Sandstone and quartzite	Fine grained polymineralic igneous crystalline rocks Andesite, dolerite, diabase and rhyolite	Coarse grained polymineralic igneous and metamorphic crystalline rocks Amphibolite, gabbro, gneiss, granite, norite and quartz diorite
Intact rock samples					
Laboratory size specimens free from joints RMR = 100 Q rating 500	$m = 7.0$ $s = 1.0$	$m = 10.0$ $s = 1.0$	$m = 15.0$ $s = 1.0$	$m = 17.0$ $s = 1.0$	$m = 25.0$ $s = 1.0$
Very good quality rock mass					
Tightly interlocking undisturbed rock with unweathered joints at 1 to 3 m RMR = 85 Q rating 100	$m = 3.5$ $s = 0.1$	$m = 5.0$ $s = 0.1$	$m = 7.5$ $s = 0.1$	$m = 8.5$ $s = 0.1$	$m = 12.5$ $s = 0.1$
Good quality rock mass					
Fresh to slightly weathered rock, slightly disturbed with joints at 1 to 3 m RMR = 65 Q rating 10	$m = 0.7$ $s = 0.004$	$m = 1.0$ $s = 0.004$	$m = 1.5$ $s = 0.004$	$m = 1.7$ $s = 0.004$	$m = 2.5$ $s = 0.004$
Fair quality rock mass					
Several sets of moderately weathered joints spaced at 0.3 to 1 m RMR = 44 Q rating 1	$m = 0.14$ $s = 0.0001$	$m = 0.20$ $s = 0.0001$	$m = 0.30$ $s = 0.0001$	$m = 0.34$ $s = 0.0001$	$m = 0.50$ $s = 0.000$
Poor quality rock mass					
Numerous weathered joints at 30 to 500 mm with some gouge. Clean compacted waste rock RMR = 23 Q rating 0.1	$m = 0.04$ $s = 0.00001$	$m = 0.05$ $s = 0.00001$	$m = 0.08$ $s = 0.00001$	$m = 0.09$ $s = 0.00001$	$m = 0.13$ $s = 0.000$
Very poor quality rock mass					
Numerous heavily weathered joints spaced < 50 mm with gouge. Waste rock with fines RMR = 3 Q rating 0.01	$m = 0.007$ $s = 0$	$m = 0.010$ $s = 0$	$m = 0.015$ $s = 0$	$m = 0.017$ $s = 0$	$m = 0.02$ $s = 0$

Notation: RMR - rock mass rating from the Geomechanics Classification;
Q - quality of rock mass from the Q-System.

From: Bieniawski, Z.T., 1984, Rock Mechanics Design in Mining and Tunneling, A.A. Balkema, Rotterdam.